Fundamentals and Applications of Gas Hydrates

Carolyn A. Koh,* E. Dendy Sloan, Amadeu K. Sum, and David T. Wu

Center for Hydrate Research, Colorado School of Mines, Golden, Colorado 80401; email: ckoh@mines.edu, esloan@mines.edu, asum@mines.edu, dwu@mines.edu

Annu. Rev. Chem. Biomol. Eng. 2011. 2:237–57

First published online as a Review in Advance on March 8, 2011

The *Annual Review of Chemical and Biomolecular Engineering* is online at chembioeng.annualreviews.org

This article's doi: 10.1146/annurev-chembioeng-061010-114152

1947-5438/11/0715-0237$20.00

*Corresponding author.

Keywords

flow assurance, energy resource, gas storage, hydrate formation, hydrate dissociation

Abstract

Fundamental understanding of gas hydrate formation and decomposition processes is critical in many energy and environmental areas and has special importance in flow assurance for the oil and gas industry. These areas represent the core of gas hydrate applications, which, albeit widely studied, are still developing as growing fields of research. Discovering the molecular pathways and chemical and physical concepts underlying gas hydrate formation potentially can lead us beyond flowline blockage prevention strategies toward advancing new technological solutions for fuel storage and transportation, safely producing a new energy resource from natural deposits of gas hydrates in oceanic and arctic sediments, and potentially facilitating effective desalination of seawater. The state of the art in gas hydrate research is leading us to new understanding of formation and dissociation phenomena that focuses on measurement and modeling of time-dependent properties of gas hydrates on the basis of their well-established thermodynamic properties.

INTRODUCTION

Gas hydrates (also known as clathrate hydrates) are solid inclusion compounds that are formed when water and gas come into contact at high pressures and low temperatures. This host-guest system comprises a host lattice of hydrogen-bonded water molecules that form cages, which encapsulate guest gas molecules such as methane, carbon dioxide, and propane (1). A detailed description of the structural properties of gas hydrates is given in the next section.

Sir Humphry Davy (2) first discovered gas hydrates in 1810 when he noticed that a solid was formed from a solution of chlorine gas (then known as oxymuriatic gas) and water above the ice point. The discovery may have even preceded Davy, as in 1778 Priestley discovered compounds (formed from freezing SO_2 in water) that may have been clathrate hydrates, but the lack of adequate documentation makes this earlier discovery uncertain (1).

Gas hydrates were not considered to have any practical relevance until 1934, when Hammerschmidt discovered that gas hydrates rather than ice were responsible for plugging gas transmission lines in Canada (3). Gas hydrates still continue to plague the oil and gas industry, as they cause a severe risk of blockages in oil and gas pipelines, both onshore and offshore (**Figure 1**). Deepwater offshore oil fields have enhanced high pressure and low temperature environments; thus, the risk of gas hydrate blockages in pipeline and offshore facilities is extreme. As such, gas hydrates are the primary problem for flow assurance, the field concerned with ensuring continuous flow of fluids in oil/gas flowlines and facilities.

Gas hydrate formation is also a key issue in deepwater oil/gas production from a safety perspective. As recently witnessed in 2010, gas hydrates were a major problem in the containment of the oil leak following the deepwater oil/gas well blowout of the Macondo well in the Gulf of Mexico. At the water depths where the oil leak was located, the temperature and pressure conditions were readily favorable for the formation of gas hydrates from the rising oil/gas plume. In fact, gas hydrate formation was the cause for the failure of a 100-ton containment structure

Figure 1

Gas hydrate plug recovered from a subsea pipeline (in a slug catcher, which stores slugs from the upstream system and is located between the outlet of the pipeline and processing equipment) off the coast of Brazil (courtesy of Petrobras).

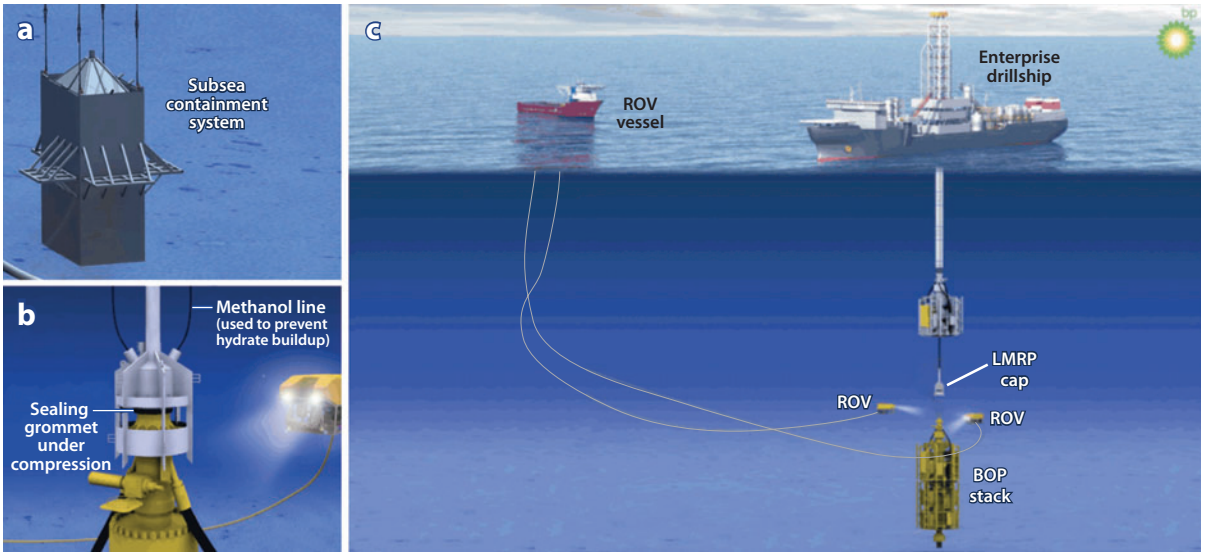

Figure 2

Deepwater Macondo well containment strategies. Original 100-ton containment structure (*a*). Lower marine riser package (LMRP) cap containment system comprising effective hydrate prevention (methanol) lines (*b,c*). ROV, remote operating vehicle; BOP, blowout preventer.

following the Macondo well blowout in the Gulf of Mexico. As such, subsequent containment of the oil leak required incorporation of effective hydrate mitigation strategies to prevent hydrate formation (see illustration in **Figure 2**).

Although gas hydrates are considered a nuisance when they occur in oil/gas flowlines, they are considered a potential asset when present in large natural deposits in arctic regions under the permafrost and in oceanic sediments along the continental margins (**Figure 3**). The global estimates of the amount of energy (methane gas) trapped within natural gas hydrate deposits varies widely, but even the most conservative estimates place the amount of energy in hydrated deposits to be twice that of all fossil fuel reserves available worldwide; upper estimates of gas hydrate deposits are orders of magnitude greater than those for natural gas reserves (4). According to the recent National Research Council report on methane hydrates (4), there are no fundamental technological hurdles to recovering energy from these natural deposits, although more research needs to be performed to determine the environmental impact of such exploration.

Other technological applications of gas hydrates include storage of natural gas and hydrogen (H_2). The ability to store natural gas in the form of gas hydrate pellets is appealing, particularly for stranded gas applications where the produced gas is too small to justify building a liquefied natural gas plant and production is too far away from a pipeline (5–7). The storage and transportation of natural gas hydrates are near commercialization; current work focuses on development and optimization for efficient production of large volumes/scale-up of gas hydrate pellets (8). Further details on the important lessons learned and heuristics for gas hydrates in energy applications, including flow assurance, energy production, and natural gas storage, are provided below.

Efforts have also been made to develop gas hydrates for hydrogen storage applications. Although hydrogen was first thought to be too small to stabilize the clathrate hydrate framework, Dyadin et al. (9) and Mao et al. (10) demonstrated that at high pressures (greater than

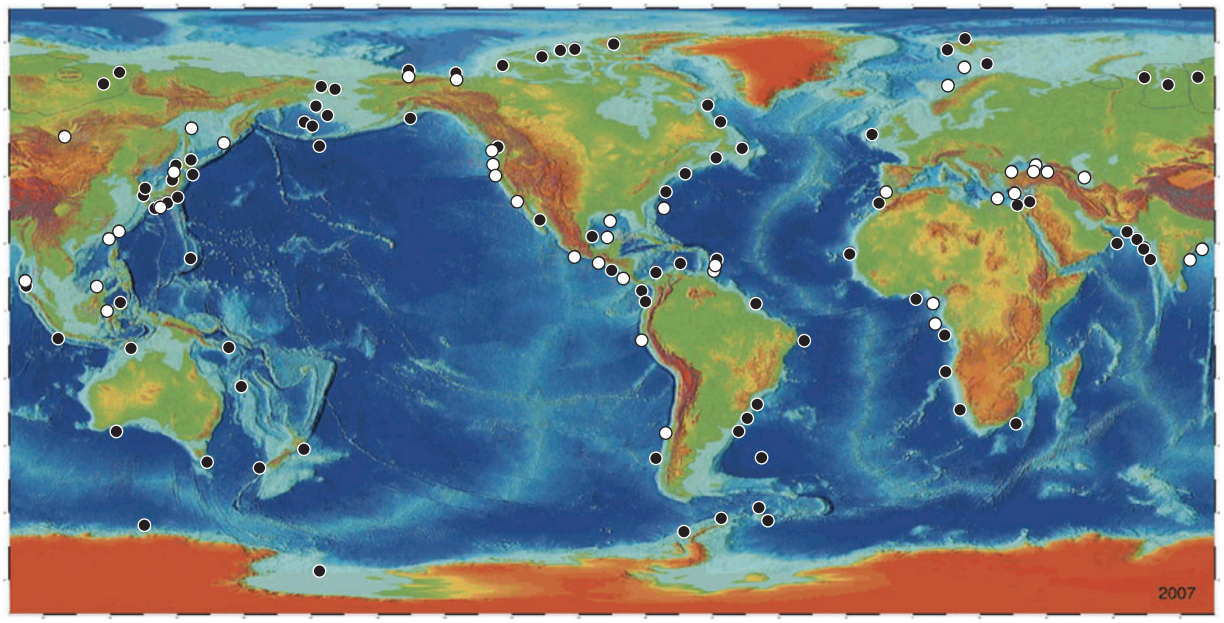

Figure 3

Global gas hydrate deposits inferred (*filled circles*) and recovered (*open circles*) in sediments along the continental margins and under the permafrost (courtesy of K. A. Kvenvolden; Reference 4).

200 MPa at room temperature), H_2 molecules can occupy the small and large cages of structure II hydrates. Promoter molecules such as tetrahydrofuran (THF) enable H_2 hydrates to be formed (and stabilized) at significantly lower pressure conditions than those required by pure H_2 hydrates. A range of promoter molecules and different clathrate structures has been used in the attempt to reduce the temperature and pressure conditions for H_2 storage (11–16). The key outstanding challenge is to store H_2 in clathrate materials at near-ambient temperature and pressure conditions as well as at high capacity (the U.S. Department of Energy target is 5.5 wt% of H_2 storage by 2015; 17).

Gas hydrates can also be applied to separation processes including separation of flue gases and desalination of seawater. In the former application, flue gases including carbon dioxide are selectively captured in gas hydrates while excluding (totally, or partially in most cases) nitrogen and other benign molecules (18). Various patents have emerged for this technological application of gas hydrates, but currently there is no clear path to commercialization. Desalination is enormously important to many countries for freshwater generation. The use of gas hydrates in the desalination process is attractive because gas hydrates will form from seawater such that salt ions are excluded (19–22). Although first suggested several decades ago (23, 24), desalination of seawater using gas hydrates is still an underexplored but potentially fruitful area requiring further research and development to investigate the technical and economic feasibility of this process.

This review examines the fundamental science and engineering knowledge base of gas hydrate structure and composition, thermodynamics, and kinetics. The state of the art of gas hydrate physics and chemistry is then incorporated into details on the lessons learned and heuristics of gas hydrate formation and decomposition in the three key energy applications of flow assurance, energy recovery, and storage materials.

GAS HYDRATE STRUCTURE AND COMPOSITION

Gas hydrates are composed of approximately 85 mol% water, and therefore many of their properties are similar to those of ice (e.g., physical appearance, refractive index, density), whereas other properties contrast greatly with those of ice (e.g., mechanical strength, heat capacity, thermal conductivity). **Table 1** compares the physical properties of the two most common hydrate structures with those of liquid water and ice. There are three main types of gas hydrate crystal structures, which are known as structure I (sI), structure II (sII), and structure H (sH). **Figure 4** shows the different hydrate structures and their associated cage types. sI comprises two different cage types, a small pentagonal dodecahedral cage, denoted 5^{12} (contains 12 pentagonal faces on the cage), and a large tetrakaidecahedral cage, denoted $5^{12}6^2$ (contains 12 pentagonal and 2 hexagonal faces on the cage). sII also includes the small 5^{12} cage in addition to a large hexacaidecahedral cage, denoted $5^{12}6^4$ (contains 12 pentagonal and 4 hexagonal faces on the cage). sH is composed of the small 5^{12} cage, a mid-sized $4^35^66^3$ cage (contains 3 square, 6 pentagonal, and 3 hexagonal faces on the cage), and a large icosahedral cage, denoted $5^{12}6^8$ (contains 12 pentagonal and 8 hexagonal faces on the cage). The type of structure formed depends primarily on the size of the guest molecule; i.e., methane fits into both the small and large cages of sI, whereas propane is too large to fit into the large cage of sI but can fit into the large cage of sII and therefore forms sII. Gas hydrates found in oil and gas pipelines are mainly sII because natural gas contains methane with small amounts of larger hydrocarbon molecules such as propane and isobutane (25). Conversely, the majority of naturally occurring deposits of gas hydrates are sI because they are composed of methane (from

Table 1 Physical properties of gas hydrates compared with those of ice[a]

Property	Water	Ice Ih	Structure I	Structure II	References
Thermal conductivity λ ($W\ m^{-1}\ K^{-1}$)	0.58 (283 K)	2.21 (283 K)	0.57 (263 K)	0.51 (261 K)	(29–31)
Thermal diffusivity κ ($m^2\ s^{-1}$)	1.38×10^{-7}[b]	11.7×10^{-7}[b]	3.35×10^{-7}	2.60×10^{-7}	(30, 32, 33)
Heat capacity C_P ($J\ kg^{-1}\ K^{-1}$)	4,192 (283 K)	2,052 (270 K)	2,031 (263 K)	2,020 (261 K)	(29, 30, 34, 35)
Linear thermal expansion at 200 K (K^{-1})	–	56×10^{-6}	77×10^{-6}	52×10^{-6}	
Compressional wave velocity, V_P ($km\ s^{-1}$)	1.5	3.87 (5 MPa, 273 K)	3.77 (5 MPa, 273 K)	3.821 (30.4–91.6 MPa, 258–288 K; C_1–C_2)	(36–39)
Shear wave velocity V_S ($km\ s^{-1}$)	0	1.94 (5 MPa, 273 K)	1.96 (5 MPa, 273 K)	2.001 (26.6–62.1 MPa, 258–288 K; C_1–C_2)	(38, 40)
Bulk modulus K (GPa)	0.015	9.09 (5 MPa, 273 K)	8.41 (5 MPa, 273 K)	8.482 (30.4–91.6 MPa, 258–288 K; C_1–C_2)	(38, 39, 41)
Shear modulus G (GPa)	0	3.46 (5 MPa, 273 K)	3.54 (5 MPa, 273 K)	3.666 (30.4–91.6 MPa, 258–288 K; C_1–C_2)	(38, 39)
Density ρ ($kg\ m^{-3}$)	999.7 (283 K)	917 (273 K)	929 (263 K)	971 (273 K); 940[c] (C_1–C_2–C_3)	(29, 36, 42, 43)

[a]Table modified from References 1 and 32; values for sI are based on CH_4 hydrate, and those for sII are based on tetrahydrofuran, CH_4-C_2H_6 (indicated by C_1–C_2), or CH_4-C_2H_6-C_3H_8 (indicated by C_1–C_2–C_3) hydrate.
[b]Calculated from $k = l/(r\ C_P)$ (32).
[c]Calculated from Reference 1.

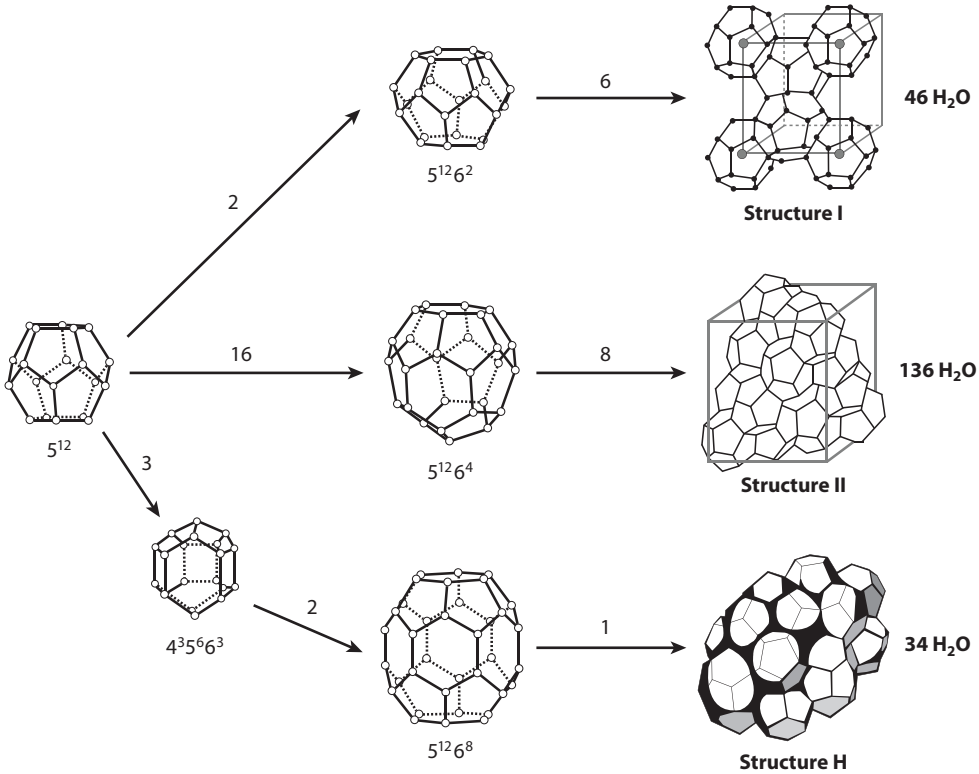

Figure 4

Common gas hydrate structures (sI, sII, sH) and the water cage types that compose the hydrate structures (47). The smallest sI repeating crystal structure is composed of 2 small 5^{12} cages and 6 large $5^{12}6^2$ cages; sII comprises 16 small 5^{12} and 8 large $5^{12}6^4$ cages; and sH contains 3 small 5^{12}, 2 mid-sized $4^3 5^6 6^3$, and 1 large $5^{12}6^8$ cages.

biogenic sources) and do not contain heavier hydrocarbons. Exceptions are thermogenic gas hydrate deposits that contain heavier hydrocarbons and therefore are formed from sII and in rarer cases sH (1, 26, 27).

Gas hydrates are known as nonstoichiometric compounds because some of the cages in the structure can be vacant; however, a sufficient number of cages must be occupied by guest molecules for the gas hydrate to be stable. Typically there is a maximum of one guest per cage, except under high pressure conditions (>0.1 GPa) when multiple occupancies of large cages can occur (e.g., high pressure H_2 and CH_4 phases; 1, 28).

The most effective techniques for confirming/characterizing the structure of gas hydrates are X-ray diffraction, Raman spectroscopy, and nuclear magnetic resonance (NMR) spectroscopy. From powder X-ray diffraction, the lattice type (sI, sII, or sH) can be readily identified. The relative cage occupancies can be determined conveniently from Raman spectroscopy, as the vibrational modes of the guest molecules provide signatures of their molecular environments (free gas, small/large cages of sI, sII). For example, the symmetric stretching mode for methane molecules trapped in hydrate cages is easily distinguished from those for methane in the free gas and liquid phases (1, 27, 44). Although qualitative information on the relative guest occupation of hydrate cages can be deduced from Raman spectroscopy, NMR spectroscopy is applied to obtain more quantitative

information on the guest(s) occupancy in gas hydrates (45). For example, solid state ^{13}C MAS (magic angle spinning) NMR spectral data for methane/ethane binary hydrates show the unique chemical shift (ppm) peak positions for each guest type occupation as well as for the free gas (46).

More sophisticated (though less accessible) tools, such as synchrotron X-ray diffraction and neutron diffraction, enable *in situ* structural characterization of gas hydrates at high pressure conditions during formation and decomposition processes (48–51). The definitive tool for structural characterization of gas hydrates is single-crystal X-ray crystallography. However, as this method requires the formation of a gas hydrate single crystal of a restricted size, which is an exceptionally challenging undertaking, only a couple of single-crystal X-ray measurements have been performed successfully (52). In a rare and remarkable case, single crystals of naturally occurring gas hydrate samples were obtained and analyzed (53).

The state of the art of structural investigations of gas hydrates is as follows:

- Gas hydrate structure can be identified by diffraction [generally considering that only known structures (sI, sII, sH) will be present].
- Guest occupancy in the cages can be elucidated with spectroscopy, although full large cage occupancy must be assumed. Carbon dioxide occupancy in a hydrate can be confirmed, though its distribution in large to small cages cannot be elucidated.
- Identification of new structures is a challenge requiring sophisticated modeling and ideally single-crystal X-ray crystallography. Although gas hydrates are typically found to be sI, sII, or sH, in some unique instances other structures are formed, such as when a large organic molecule is combined with a gas hydrate former; e.g., TBAB (tetrabutylammonium bromide) + methane produces a semiclathrate structure. TBAB participates as part of the host lattice, hydrogen bonding with water, and also as a guest (11). A novel structure HS-1 (1.67 choline hydroxide • tetra-*n*-propylammonium fluoride • 30.33 H_2O, in which the choline guest exhibits hydrophobic and hydrophilic modes of hydration) has been revealed that comprises alternating stacking layers of sH and sII hydrates (54). It is reasonable to assume that other gas hydrate structures can form, though their identification may not have been realized yet or remains a challenge.
- Metastable gas hydrate phases, which precede the thermodynamically stable structure, can exist for prolonged periods (48, 55).

THERMODYNAMICS OF GAS HYDRATES

A clear understanding of the thermodynamic properties of gas hydrate systems is critical in all gas hydrate applications, from determining the temperature and pressure conditions at which a pipeline will be within the hydrate stability zone, to assessing the conditions necessary to dissociate a gas hydrate plug in a pipeline or a natural gas hydrate reservoir for energy production, to simply establishing the conditions at which a gas hydrate system can be synthesized in the laboratory. Gas hydrate stability depends on temperature, pressure, gas composition, and condensed phase composition (including liquid hydrocarbon phase, salt content, and chemical inhibitor concentration). **Figure 5** illustrates the pressure and temperature profile to which fluids can be subjected within an oil/gas pipeline from a deepwater well to the platform and central processing facility. The shaded envelope is the hydrate formation/stability region; any fluid within the pipeline section in this region can form gas hydrates, which could result in hydrate plug formation.

As indicated in **Figure 5**, adding a chemical inhibitor such as methanol (or monoethylene glycol), typically called a thermodynamic inhibitor, will result in the hydrate stability zone shifting to colder temperatures and/or higher pressures. As an example, adding 30 wt% methanol in this case will shift the hydrate stability curve to the left such that the previously hydrate-prone pipeline

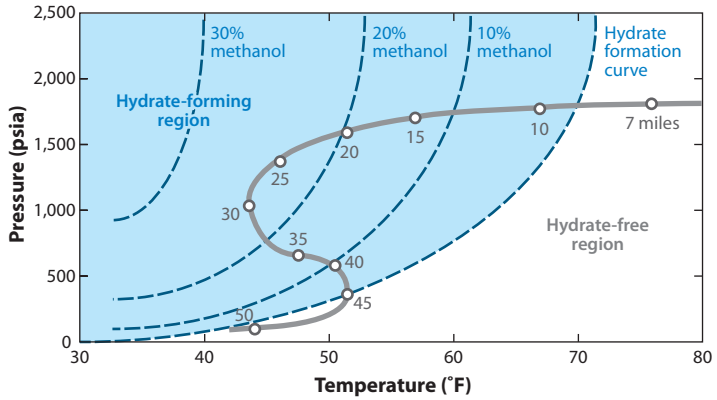

Figure 5

Schematic of the pressure and temperature conditions of fluids (gas/water/oil) in a subsea pipeline and the gas hydrate formation/stability region.

section illustrated here will no longer be within the hydrate stability zone, and therefore hydrates will be prevented from forming. This methodology of preventing gas hydrate formation using thermodynamic inhibition is also known as gas hydrate avoidance. Other thermodynamic methods to inhibit gas hydrate formation include heating/insulating the pipeline section(s) above the gas hydrate formation temperature or operating naturally with a high-salt-content fluid (1, 25).

Gas hydrate thermodynamic stability depends on the fluid composition and in particular on the gas composition. For example, the addition of a larger molecule, such as propane to methane, will result in the mixed gas hydrate (containing methane + propane guest molecules) forming at significantly lower pressure (milder conditions) than pure methane hydrate. That is, at 277.6 K, the formation pressure for pure propane hydrate (sII) is 4.3 bar, for pure methane hydrate (sI) is 40.6 bar, and for a methane + propane hydrate (50:50 binary gas mixture) is approximately 8.0 bar. As noted above, propane stabilizes the large cage of sII but is too large to fit into the large cage of sI (and can also form as pure propane hydrate). Therefore, a methane + propane gas mixture (with >0.01 mol% propane) will form sII hydrate, whereas pure methane forms sI hydrate. In the case of methane + ethane gas mixtures, although each guest type forms sI alone, at specific binary gas compositions and pressures, binary sII hydrate or binary sI hydrate can be formed alone, or sI and sII binary hydrates can coexist (1).

The effect of propane in a methane + propane system is analogous to the promoter molecule effect that is exploited in gas storage applications to reduce the pressure conditions for hydrate stability. In this case, the promoter molecule can stabilize the hydrate structure at lower pressures than can the fuel gas molecule (methane, natural gas, or H_2). For example, THF (which is similar to propane) stabilizes the large cage of sII, and alone will form sII hydrate at atmospheric pressure at temperatures below 277.5 K. Therefore, by adding THF to methane or hydrogen, the hydrate stability pressure can be significantly reduced (56, 57).

Gas hydrate thermodynamic prediction models (of the gas hydrate phase boundary) are currently mostly based on the original van der Waals-Platteeuw (vdWP) theory (1, 58), which in turn is based on the key idea of estimating the free energy of the hydrate as that of a framework of water cages that can absorb guests individually and independently. This free energy is then compared with that of the coexisting phases to determine the phase boundary.

The vdWP theory can be considered to consist of a set of key assumptions about the nature of molecular interactions plus methods to estimate the parameters that characterize the strength

of these interactions. Specifically, the commonly cited central assumptions are (*a*) independence of the free energy of the water framework from the guest occupancy (sometimes described as the guest not distorting the water lattice), (*b*) single occupancy of cages, (*c*) lack of guest-guest interactions, and (*d*) no quantum effects (valid for all but the lightest guests). These assumptions lead to a relatively simple form for the chemical potential of water in a lattice with guest molecules, relative to a hypothetical empty lattice [hydrate (H), water (W)]:

$$\Delta\mu_{\mathrm{W}}^{\mathrm{H}} = -kT \sum_{m} \nu_m \ln\left(1 - \sum_{i} \Theta_{mi}\right), \qquad 1.$$

where ν_m is the number of cages of type m in the unit cell, T is the absolute temperature, k is Boltzmann's constant, and the fractional occupancy of guest species i in hydrate cages of type m is given by

$$\Theta_{mi} = \frac{C_{mi} f_i}{1 + \sum_{i} C_{mi} f_i}, \qquad 2.$$

where C_{mi} is the Langmuir constant for guest species i in cages of type m, and f_i is the gas phase fugacity of guest species i. The original vdWP theory estimates the Langmuir constant, a measure of the guest-water interaction strength, by making further simplifying assumptions that this interaction can be modeled as pairwise and short range between a freely rotating guest in a single spherical cavity.

Although many of the specific assumptions have been shown to be individually quantitatively inaccurate, the success of the vdWP theory in large part lies in the robustness of the form of Equations 1 and 2 to relaxing the assumptions above. For instance, long-range guest-water interactions as well as deformations of the lattice can be incorporated into an effective Langmuir constant; these and related effects do not change the form of the equations as long as these guest-water interactions are independent from each other. Recent advances in molecular simulation have allowed careful dissection of the accuracy of specific assumptions of the vdWP model and have in addition concluded that the accuracy of the original theory was due in part to cancellation of errors from individual assumptions (59). Naturally, the accuracy of the model improves if the Langmuir constants are fit to experimental data, and such semiempirical models provide the best fits, at least for temperature and pressure.

Several of the current models include various modifications of the vdWP theory such as extending the model to multicomponent gas mixtures (61), accounting for lattice expansion due to guest occupation (60, 62), and implementing a Gibbs energy minimization model, which is the basis of the thermodynamic hydrate prediction model called CSMGem (CSM Gibbs energy minimization model) (62, 63). Molecular (Monte Carlo, MC) simulations have also been applied to compute hydrate thermodynamics; these simulations can independently evaluate the vdWP method and determine the gas hydrate phase boundary from knowledge only of the intermolecular potentials/interactions of the guest and host molecules (59, 64, 65).

Figure 6 compares the accuracy of several different hydrate thermodynamic prediction software packages against many data sets measured for a wide range of gas hydrate systems. This comparison demonstrates that the incipient hydrate temperature and pressure can be predicted to within the experimental accuracy of the measurements, i.e., 0.65 K and 10% of overall pressure, respectively. Similarly, comparisons of predictions and experiments for inhibited hydrate systems (i.e., gas + water systems containing methanol and NaCl) are accurate to within approximately 2 K and 20% of overall pressure.

Experimental methods for measuring phase equilibria of hydrates as well as tables of systems investigated can be found in review papers (66, 67). In some more specialized applications, such

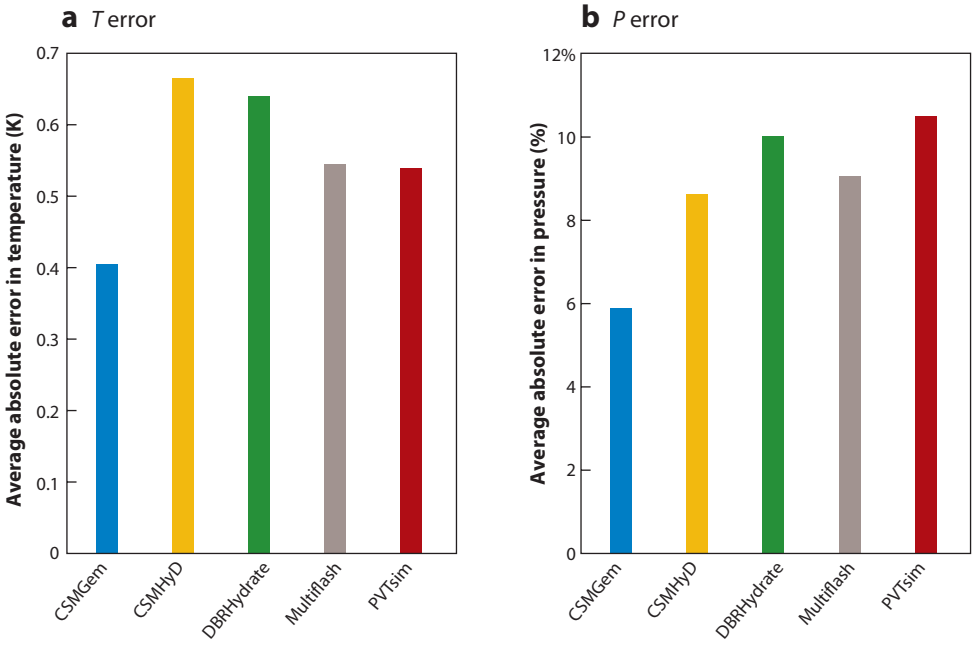

Figure 6

Comparison of the uninhibited incipient hydrate temperature (*T*) and pressure (*P*) errors (absolute) for natural gas hydrates (1,685 data points) using several different gas hydrate thermodynamic prediction software packages: a Gibbs energy minimization program, CSMGem; an earlier CSM hydrate program, CSMHyD; and commercial packages including DBRHydrate from DBR-Schlumberger, Multiflash from Infochem, and PVTSim from Calsep (1).

as for gas fields containing high concentrations of hydrogen sulfide (H_2S), there is a need to produce new reliable gas hydrate experimental data, which are limited; further measurements are also required to validate predictive models. However, apart from such specific applications, one can conclude that the thermodynamic properties of gas hydrates (phase equilibria) are sufficiently well characterized to enable the state of the art in gas hydrate research to focus on developing our understanding of time-dependent hydrate phenomena.

TIME-DEPENDENT PROPERTIES OF GAS HYDRATES

Unlike the well-established thermodynamic properties of gas hydrates, the kinetics of gas hydrate formation remains a challenge. That is, predictions, and even measurements, of the rate of gas hydrate formation are difficult and unresolved owing to problems with obtaining reproducible and instrument-independent kinetic data. The stochastic (random) nature of hydrate formation is commonly observed in laboratory-scale experiments, where the nucleation induction time can vary under identical test conditions from minutes to hours to days. The nucleation induction time is typically defined as the time up to the point when hydrate growth occurs spontaneously, which in practice is usually taken as the time that produces measurable changes such as pressure decrease, gas consumption, temperature rise, or crystals that can be observed visually.

The ability to control and/or predict the kinetics of gas hydrate formation is important in preventing gas hydrate plug formation during risk management strategies. Risk management is

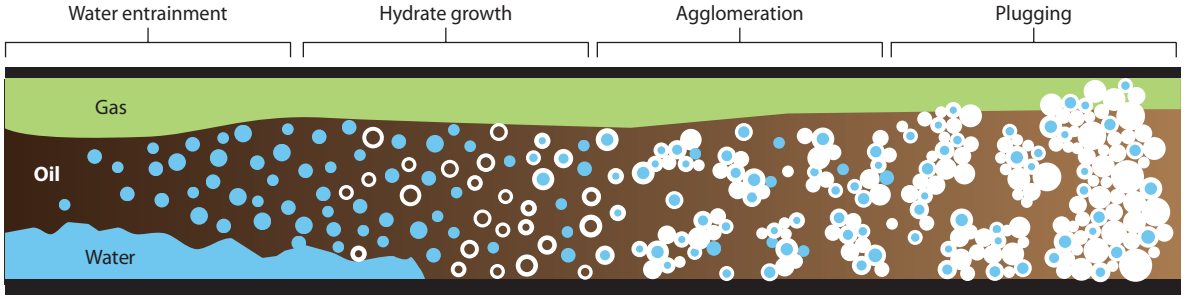

Figure 7

Conceptual picture of hydrate formation in a multiphase flow line used in the CSM Hydrate Kinetic model, CSMHyK.

typically used when thermodynamic avoidance is uneconomical and/or technically unfeasible, e.g., requiring large amounts of methanol (>40 to 60 vol%), or when umbilicals have limited methanol injection capacity. Risk management strategies include controlling the time-dependent properties of gas hydrates.

The ability to predict when gas hydrates will form in a flowline is extremely valuable to exploration field design and developments and is the focus of a unique state-of-the-art tool, CSMHyK (CSM Hydrate Kinetic model), which is coupled to an industrial standard multiphase flow simulator, OLGA® from the SPT Group. The conceptual picture for hydrate formation in an oil-dominated pipeline that is used in version 1.0 of the CSMHyK model is illustrated in **Figure 7**. Initially, water droplets are entrained in the continuous oil phase owing to shear in the pipeline and often also because of surface-active agents in the oil phase (68). Hydrate nucleates and grows at the water interface (which is in contact with gas dissolved in oil) to form a hydrate shell around the droplet. The hydrate particles agglomerate owing to capillary attraction (69, 70) and eventually jam and plug the pipeline (1, 71–73).

A key input parameter in CSMHyK is the subcooling ($T_{eq} - T_{system}$) at which hydrate starts to form, which has been empirically determined to be 3.6 K. This value was first suggested by Matthews & Notz (74) when evaluating the subcooling required for hydrate formation during Texaco flowloop tests and the Werner-Bolley gas condensate field test. Given the enormous investment and efforts required for hydrate field tests, the Werner-Bolley field test remains the most controlled and documented one for gas hydrate plug formation. Since this time, numerous flowloop tests (at the ExxonMobil and Tulsa University flowloop facilities) have demonstrated that the subcooling temperature at which hydrates form is 3.6 ± 0.3 K.

CSMHyK-OLGA® has been used to predict gas hydrate formation in flowloop and field tests. A scaling of 1/500 of the intrinsic kinetic rate constant for methane hydrate formation (75), reflecting the need to account for mass and heat transfer rate-limiting effects, was determined by fitting CSMHyK predictions to one oil in the ExxonMobil flowloop. The same fit was found to successfully predict hydrate formation in two different flowloops for four different oils. CSMHyK also predicted hydrate plug formation data obtained in the Tommeliten Gamma field test (73).

The ultimate goal for designed kinetic control of hydrates in pipelines (as well as in clathrate hydrate storage materials) is to elucidate the detailed mechanisms of hydrate formation and design chemical inhibitor molecules (or promoter molecules) to target key kinetic pathways. Over the past few years, elucidation of the mechanism of hydrate formation has been accelerated owing to the development of high performance supercomputing power. The first microsecond-scale computer simulations of methane hydrate nucleation and growth have revealed new insights into a possible mechanism for these processes (76; **Figure 8*a***).

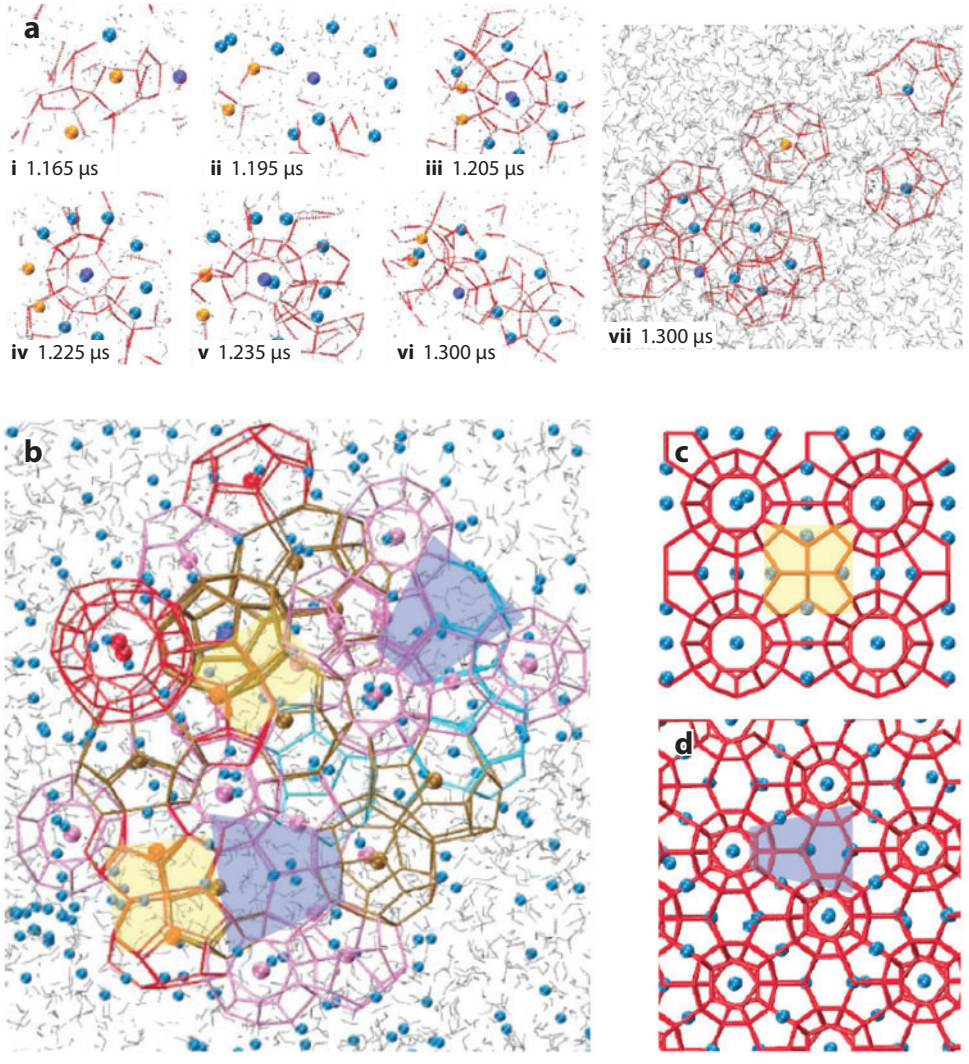

Figure 8

(*a*) Microsecond-scale computer simulations revealing a mechanism of methane hydrate nucleation. (*b–d*) sI/sII motifs linked by $5^{12}6^3$ cages in the final methane hydrate structure (76).

From these simulations the suggested mechanism involves the following key steps: (*i*) dissolved methane molecules increase the chances of shared planar water rings forming; (*ii*) the initial structure gradually forms partial and complete hydrate cages, and methane adsorbs onto (coats and protects) the planar faces of the cages and induces local order; and (*iii–vii*) the initial cages fluctuate owing to dynamic hydrogen bonding, with the small 5^{12} cages dominating. **Figure 8*b–d*** shows that the final structure has a mixture of sI/sII motifs, with $5^{12}6^3$ linking cages facilitating this structure coexistence (*cf.* 77). The sI/sII coexistence identified in these computer simulations of hydrate formation is consistent with experimental observations reported by Schicks & Ripmeester (78) and also by Murshed & Kuhs (48) and Ohno et al. (55); in the last study sI/sII mixtures were formed before converting to thermodynamically preferred phases.

New insights obtained from such large-scale computer simulations of the molecular pathways to gas hydrate formation could be utilized in the future to facilitate molecular engineering and design of the control processes and chemicals for enhanced gas hydrate inhibition and/or promotion, which are key concerns in the energy applications of gas hydrates.

ENERGY APPLICATIONS

For hydrate formation, four ingredients are jointly required: (*a*) small guest molecules (<0.9 nm diameter), (*b*) water (in any physical state), (*c*) relatively low temperature (typically <323 K), and (*d*) high pressure (typically 2 to 1,000 MPa). Without any one of the four, gas hydrates cannot exist. However, those four components are typically present in natural gas and oil production, and thus gas hydrate crystals jeopardize fluid flow. When oil is produced, almost invariably natural gas and water are also produced at high pressure, whereas pipelines often are at low temperature. Low temperatures are unavoidable, for example, in winter or arctic conditions, or at ocean depths greater than 600 m, where the temperature is approximately uniform at 277 K.

Because hydrate crystals can plug flowlines, resulting in days and sometimes weeks of lost production, there is substantial incentive to avoid hydrates by removal of one of the four components despite the expense. Avoidance of hydrate plugs in flowlines is achieved (in parallel with the four above requirements) through four methods:

1. Dead oil—oil without dissolved smaller molecules—is frequently circulated in a flowline until the line has warmed above the hydrate formation temperature.
2. Both free and dissolved water are removed using separators followed by glycol or molecular sieve drying towers. Inhibitors such as alcohols and glycols are injected into flowlines to compete with hydrates for available free water (through hydrogen bonding). Inhibitor injection requires lower temperatures and/or higher pressures for hydrate formation.
3. Onshore, it is possible to produce gas at the wellhead so that reservoir temperatures are retained above hydrate formation conditions until the hydrocarbon reaches the point of water removal.
4. The economics of high energy density normally prevents low pressure operation of flowlines. However, when hydrate plugs do form in flowlines, depressurization provides hydrate temperatures below those of the environment, resulting in radial dissociation due to heat flow.

As an example mechanism by which hydrate plugs form, consider a flowline producing gas, oil, and water in the deep (>600 m) ocean. At the inlet, both the pressure and the temperature are high, retaining the reservoir thermal energy. However, within a short distance from the wellhead, the temperature cools to 277 K, usually with only a small pressure drop, so the system enters the hydrate formation stability region. Water (usually brine) produced from the reservoir as well as condensed freshwater accumulate at low-lying points in the flowline. When the gas and oil bubble through the accumulated water, their exit creates substantial surface area in the form of bubbles and foams. If the cold water is uninhibited, hydrated bubbles of gas will form and aggregate into a plug just downstream of the accumulated water. Although other mechanisms of gas hydrate plug formation exist (25, chapter 2) the resulting plugs have the same effect—no flow.

Figure 9 shows a time sequence of hydrate plug formation from methane (the major component of natural gas) bubbling through water in a sight glass at 6.7 MPa and 277 K. In the first frame (*a*), the water layer is below the gas in the chamber; in the middle frame (*b*) a small aggregation of hydrate-encrusted gas bubbles appears at the interface, which grows to a more substantial plug in the last frame (*c*). Such a picture also might be representative of a plug at a collection vessel from a deepwater well blowout (*cf.* **Figure 2**).

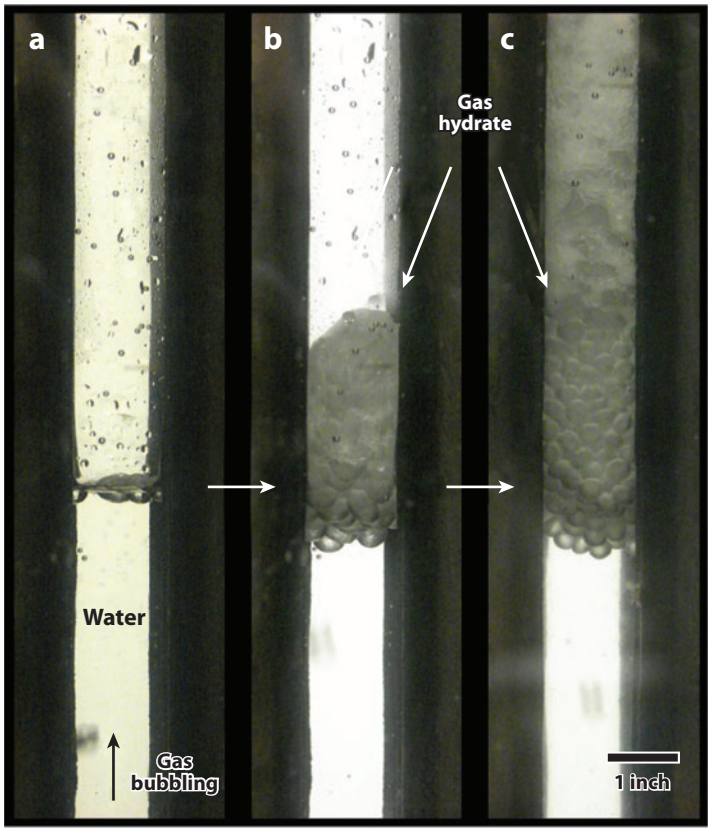

Figure 9

The aggregation of hydrate-encrusted gas bubbles at an interface. The white arrows indicate the passage of time from no hydrates to a hydrate plug.

Hydrate plugs anneal and harden with time, inhibiting fluid flow. Unlike plugs of other materials such as wax, asphaltenes, or scale, which require days or weeks to form, hydrate plugs aggregate in minutes but require emergency remediation for days, weeks, or sometimes months. It is this situation that all flow assurance engineers seek to avoid, and why hydrates rank as the principal flow assurance problem in deepwater oil/gas production. Happily, unlike flowline blockages with other materials, industry has no recorded incident of abandonment of a flowline owing to a hydrate plug.

After the hydrate plug location and length are determined, remediation requires removal of one or more of the four requirements, usually via depressurization of the pipeline, but also through injection of inhibitors at the plug face/annulus, careful thermal heating, or sometimes mechanical removal using coiled tubing. Safety precautions are observed in plug removal (25, chapter 3) for two reasons. First, during depressurization, the most common removal technique, the flowline plug temperature is below that of the surroundings, so radial detachment occurs first at the wall; any preexisting pressure gradient will cause the plug to become a flowline projectile, sometimes with disastrous consequences. Second, if a flowline is heated, large volumes of gas evolve (164 volumes of gas at standard temperature and pressure for every volume of dissociated hydrate), which requires gas release at the plug terminals to prevent line overpressure.

Because plug remediation is so expensive from both safety and lost production perspectives, substantial effort is spent on plug prevention. In addition to the above avoidance techniques, which have been in common practice since the initial flowline hydrate plug discovery in 1934, new risk management techniques have arisen since 1990, largely owing to low dosage hydrate inhibitors (LDHIs). In these techniques small hydrate particle formation is encouraged, but aggregation to large plugs is avoided via kinetic and agglomeration prevention. In kinetic inhibition, crystal nucleation and growth are prevented by anchoring polymers at the small crystal surface, which provides a barrier to crystal growth that is overcome only at higher (>10°C) subcooling. In the second technique, antiagglomerants prevent the aggregation of small hydrate particles to form a plug, enabling flow of particles with the oil phase (79). Although avoidance techniques remain the norm in industry, risk management methods are becoming accepted to enable tenuous production to become economical.

Energy Recovery

Large natural gas hydrate deposits have resulted in programs to recover this hydrocarbon resource. **Figure 10** shows four hydrated deposit samples: At left are two from permafrost regions in Canada (**Figure 10*a***) and Alaska (**Figure 10*b***), and at right are two from the ocean in India (**Figure 10*c***) and off Canada (**Figure 10*d***).

A review paper (80) summarizes the state of the art of hydrated gas recovery. **Figure 11*a*** shows the relative amount of hydrated gas relative to conventional gas reserves, indicating that

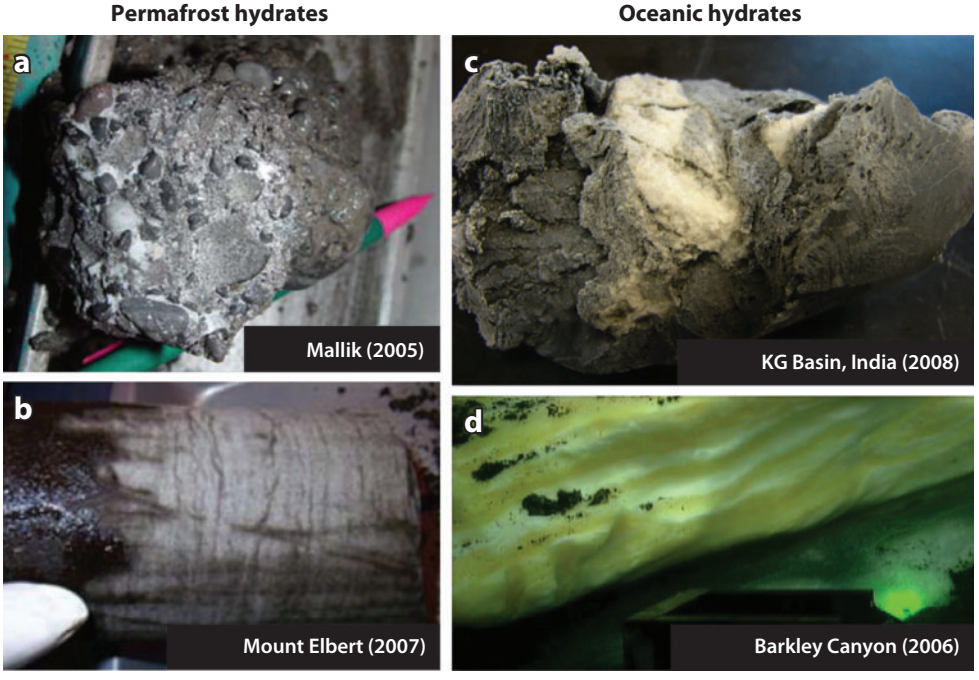

Figure 10

Four hydrated samples. At left are two from the permafrost regions in Canada (*a*) and Alaska (*b*) (used with permission from R. Boswell and T. Collett); at right are ocean samples from India [Krishna Godavari (KG) Basin, *c*] and Canada (*d*).

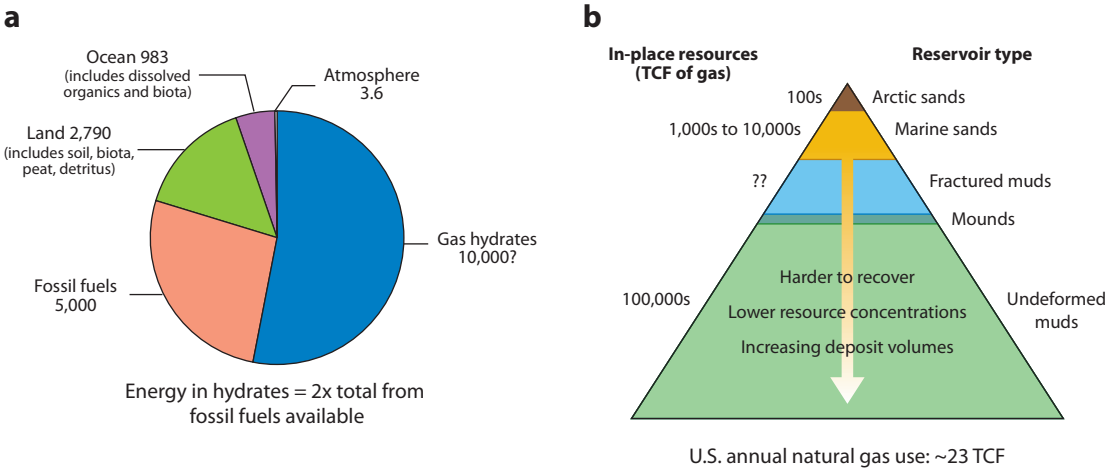

Figure 11

(*a*) A comparison of energies in conventional hydrocarbons and hydrates. The distribution of organic carbon in Earth reservoirs is shown in gigatons (10^{15} tons) of carbon. 1 gigaton = 38.84 trillion ft^3 (TCF). (*b*) A comparison of hydrated resources and the difficulty of recovery, which increases as production progresses to the silts and undeformed muds shown lower in the diagram. The estimated global amount of methane in gas hydrate deposits is 700,000 TCF; the U.S. annual natural gas use is ~23 TCF. Adapted from Reference 84 with permission from AAAS.

there is twice as much hydrated gas as there is gas in all other hydrocarbon reserves combined. **Figure 11*b*** shows that gas hydrate deposits contain 700,000 trillion ft^3 (TCF) of methane relative to the U.S. annual natural gas usage of 23 TCF.

Four points should be noted about **Figure 11**:

1. Almost all of the hydrated energy is in the ocean, so much so that errors in the oceanic hydrate estimate can overshadow the hydrated gas in the permafrost regions.
2. The most approachable natural hydrates are located in small, concentrated permafrost deposits. Proof of concept for hydrated gas production was performed in 2007 and 2008 in the permafrost. The first long-term permafrost hydrate production tests will be done in 2012 to assess methods of production and geomechanical effects, to provide data to correct models, and to provide a basis for technology transfer to ocean production.
3. In the oceans, the most producible deposits are those hydrates in sandy sediments. The majority of hydrate deposits in silt (shown in **Figure 11*b***) are not thought to be producible (81).
4. Hydrated gas production technology is currently precommercial but aggressively pursued by Japan, China, India, Korea, Taiwan, and the United States (1, 4). Japan has an initial goal of producing gas from hydrates by 2015.

Stranded Gas Transport via Hydrates and Hydrate Slurries

Approximately 70% of the world's gas is defined as stranded—too small to justify a liquefaction facility and too far away from a pipeline. Gudmundsson & Parlaktuna (82) first suggested hydrated storage and shipping of natural gas; subsequent publications from the Gudmundsson laboratory (6, 7) developed this idea further.

The concept was given more impetus by Stern et al. (83), who discovered an anomalous self-preservation effect of hydrates that suggested only mild refrigeration (268 K) was required

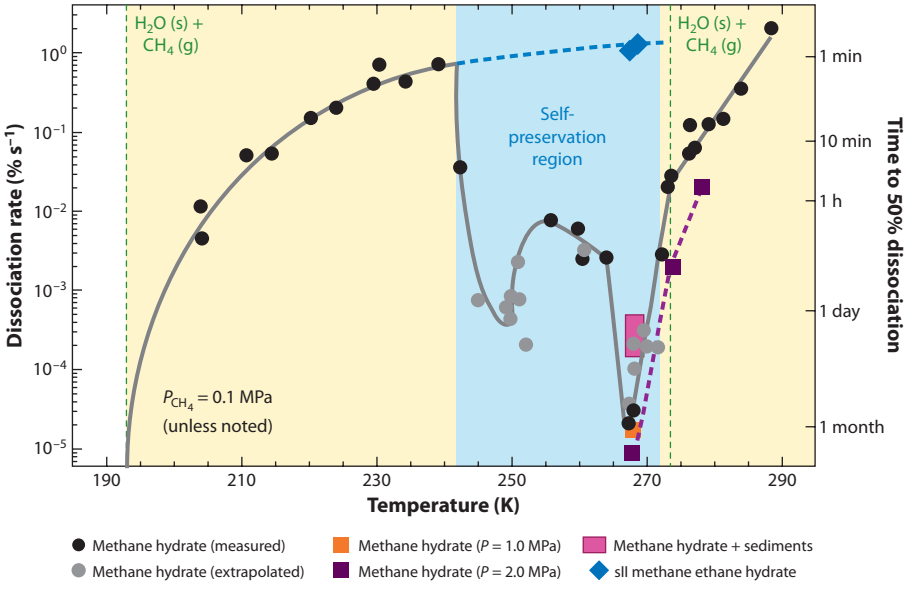

Figure 12

Self-preservation of hydrates (dissociation rate on left ordinate, and time for 50% dissociation on right) as a function of temperature. The extrapolated time is shown as a dashed line versus the black points representing observations in the self-preservation region. Figure courtesy of L. Stern.

to preserve the hydrates for longer periods at atmospheric pressure. This result is shown in **Figure 12**; the data suggest that at 268 K, 50% of the hydrate could survive for one month; when extrapolated, the expected 50% survival time was a few minutes. Because these phenomena are not present above the ice point, ice seems to play a role in self-preservation.

Mitsui Shipbuilding & Engineering Company has a 5,000 ton day^{-1} pilot plant close to their liquefied natural gas offloading facility in Hiroshima and plans to scale up to a 100,000 ton day^{-1} facility to enable this technology. The topic of natural gas hydrate storage in slurries is currently an active area of interest by industry.

CONCLUSIONS

This article has examined the state-of-the-art knowledge base of gas hydrates. The structural and physical properties of gas hydrates are largely well characterized (though hydrate-bearing sediment systems are less well defined). The structural properties of gas hydrates (and hence gas composition) play an important role in the thermodynamic properties of these compounds. As thermodynamic prediction tools are accurate to within experimental measurement accuracy in most cases, the research focus is moving to time-dependent studies of gas hydrates. This shift in focus is key to all applications of gas hydrates, from the pipeline issue of preventing hydrate plugs from forming, to processes involved in energy recovery or storage.

New advances in gas hydrate science and engineering are pushing the frontiers of research to more challenging and sophisticated areas of time-dependent gas hydrate properties as well as to molecular engineering design of gas hydrate control strategies. These advances are accompanied by requirements to control gas hydrate formation under more extreme environments of deepwater drilling and exploration where pressures can exceed several tens of MPa and even approach

100 MPa in some cases; also energy recovery from hostile environments several thousands of meters under the permafrost and/or deep oceans present conditions where hydrate reformation will be prevalent. The benefits of developing new methods to control hydrate formation and dissociation processes can be enormous, including avoiding hydrate plug formation during development of deepwater oil/gas fields, promoting hydrate slurry flow during subsea oil/gas transportation, recovering the enormous energy prize trapped within deep natural hydrate deposits, and facilitating effective storage of fuel within the hydrate lattice. Among all these advanced technological applications of gas hydrate engineering, safety is by far the most important consideration, in terms of personnel, equipment and environmental safety and impacts.

DISCLOSURE STATEMENT

The authors are not aware of any affiliations, memberships, funding, or financial holdings that might be perceived as affecting the objectivity of this review.

ACKNOWLEDGMENTS

The authors acknowledge financial support by the Center for Hydrate Research Consortium (BP, Chevron, ConocoPhilips, ExxonMobil, Nalco, Petrobras, Schlumberger, Shell, Statoil, and Total). Funding from NSF-MRI (CBET-1053590) is also acknowledged.

LITERATURE CITED

1. Sloan ED, Koh CA. 2008. *Clathrate Hydrates of Natural Gases*. Boca Raton: CRC Press. 721 pp. 3rd ed.
2. Davy H. 1811. The Bakerian Lecture. On some of the combinations of oxymuriatic gas and oxygene, and on the chemical relations of these principles to inflammable bodies. *Philos. Trans. R. Soc. London* 101:1–35
3. Hammerschmidt EG. 1934. Formation of gas hydrates in natural gas transmission lines. *Ind. Eng. Chem.* 26:851–55
4. Paull C, Dallimore SR, Enciso G, Green S, Koh CA, et al. Comm. Assess. Dept. Energy's Methane Hydrate Res. Dev. Prog.: Eval. Methane Hydrate Future Energy Resour. 2010. Realizing the energy potential of methane hydrate for the United States. *Natl. Acad. NRC Rep.*, Washington DC: Natl. Acad. Press
5. Andersson V, Gudmundsson J. 2000. Flow properties of hydrate-in-water slurries. *N. Y. Acad. Sci.* 912:322–29
6. Gudmundsson JS, Andersson V, Levik O, Mork M. 2000. Hydrate technology for capturing stranded gas. *N. Y. Acad. Sci.* 912:403–10
7. Gudmundsson JS, Mork M, Graff OF. 2002. Hydrate non-pipeline technology. *Proc. Intl. Conf. Gas Hydrates, 4th*, Yokohama, Japan, pp. 997–1102. Tokyo: Keio Univ.
8. Watanabe S, Takahashi S, Mizubayashi H, Murata S, Murakami H. 2008. A demonstration project of NGH land transportation system. *Proc. Intl. Conf. Gas Hydrates, 6th, Vancouver*. CD-ROM.
9. Dyadin YA, Larionov EG, Manakov AY, Zhurko FV, Aladko EY, et al. 1999. Clathrate hydrates of hydrogen and neon. *Mendeleev Commun.* 9:209–10
10. Mao WL, Mao H-K, Goncharov AF, Struzhkin VV, Guo Q, et al. 2002. Hydrogen clusters in clathrate hydrate. *Science* 297:2247–49
11. Chapoy A, Anderson R, Tohidi B. 2007. Low-pressure molecular hydrogen storage in semi-clathrate hydrates of quaternary ammonium compounds. *J. Am. Chem. Soc.* 129:746–47
12. Prasad PSR, Sugahara T, Sum AK, Sloan ED, Koh CA. 2009. Hydrogen storage in double clathrates with *tert*-butylamine. *J. Phys. Chem. A* 113:6540–43
13. Shin K, Kim Y, Strobel TA, Prasad PSR, Sugahara T, et al. 2009. Tetra-*n*-butylammonium borohydride semiclathrate: a hybrid material for hydrogen storage. *J. Phys. Chem. A* 113:6415–18

14. Sugahara T, Haag JC, Prasad PSR, Warntjes AA, Sloan ED, et al. 2009. Increasing hydrogen storage capacity using tetrahydrofuran. *J. Am. Chem. Soc.* 131:14616–17
15. Sugahara T, Haag JC, Prasad PSR, Warntjes AA, Sloan ED, et al. 2009. Large-cage occupancies of hydrogen in binary clathrate hydrates dependent on pressure and guest concentration. *J. Phys. Chem. C* 114:15218–22
16. Tohidi B, Yang J, Chapoy A, Arjmandi M, Anderson RA. 2006. *World Patent No. WO2006/131,738*
17. U.S. Dept. Energy. 2010. *Hydrogen storage*. **http://www1.eere.energy.gov/hydrogenandfuelcells/storage/current_technology.html**
18. Kang S-P, Lee H. 2000. Recovery of CO_2 from flue gas using gas hydrate: thermodynamic verification through phase equilibrium measurements. *Environ. Sci. Technol.* 34:4397–400
19. Max MD, Pellenbarg RE. 1999. *U.S. Patent No. 5,873,262*
20. Max MD, Pellenbarg RE. 2000. *U.S. Patent No. 6,158,239*
21. Max MD. 2003. *U.S. Patent No. US2003/0024803 A1*
22. Max MD. 2005. *U.S. Patent No. US2005/0184010 A1*
23. Barduhn AJ. 1967. Desalination by crystalline processes. *Chem. Eng. Progr.* 63:98–103
24. Knox WG, Hess M, Jones GE, Smith HB. 1961. The hydrate process. *Chem. Eng. Progr.* 57:66–71
25. Sloan ED, Sum AK, Koh CA, Creek JL, Ballard A, et al. 2010. *Natural Gas Hydrates in Flow Assurance*. New York: Elsevier. 200 pp.
26. Lu H, Seo Y, Lee J, Moudrakovski I, Ripmeester JA, et al. 2007. Complex gas hydrate from the Cascadia margin. *Nature* 445:303–6
27. Hester KC. 2007. *Probing hydrate stability and structural characterization of both natural and synthetic clathrate hydrates*. PhD thesis. Colo. Sch. Mines, Golden, Colo. 293 pp.
28. Hirai H, Tanaka T, Kawamura K, Yamamoto Y, Yagi T. 2004. Structural changes in gas hydrates and existence of a filled ice structure of methane hydrate above 40 GPa. *J. Phys. Chem. Solids* 65:1555–59
29. Weast RC. 1987. *CRC Handbook of Chemistry and Physics*. Boca Raton: CRC Press. 68th ed.
30. Waite WF, Gilbert LY, Winters WJ, Mason DH. 2005. Thermal property measurements in THF hydrate and hydrate-bearing sediment between −25 and +4°C, and their application to methane hydrate. *Proc. Intl. Conf. Gas Hydrates, 5th, Trondheim, Norway.* 5:1724–33, Trondheim: Tapir Acad. Press
31. Huang D, Fan S. 2004. Thermal conductivity of methane hydrate formed from sodium dodecyl sulfate solution. *J. Chem. Eng. Data* 49:1479–82
32. Waite WF, Santamarina JC, Cortes DD, Dugan B, Espinoza DN, et al. 2009. Physical properties of hydrate-bearing sediments. *Rev. Geophys.* 47:RG4003
33. Turner DJ, Kumar P, Sloan ED. 2005. A new technique for hydrate thermal diffusivity measurements. *Int. J. Thermophys.* 26:1681–91
34. Leaist DG, Murray JJ, Post ML, Davidson DW. 1982. Enthalpies of decomposition and heat capacities of ethylene oxide and tetrahydrofuran hydrates. *J. Phys. Chem.* 86:4175–78
35. Handa YP. 1986. Compositions, enthalpies of dissociation, and heat capacities in the range 85 to 270 K for clathate hydrates of CH_4, C_2H_6, C_3H_8, and enthalpy of dissociation of i-C_4H_{10} hydrate, as determined by a heat-flow calorimeter. *J. Chem. Thermodyn.* 18:915–21
36. Lee MW, Hutchinson DR, Collett TS, Dillon WP. 1996. Seismic velocities for hydrate bearing sediments using weighted equation. *J. Geophys. Res.* 101:20347–58
37. Mavko G, Mukerji T, Dvorkin J. 1998. *The Rock Physics Handbook: Tools for Seismic Analysis in Porous Media*. Cambridge, UK: Cambridge Univ. Press. 329 pp.
38. Helgerud MB, Waite WF, Kirby SH, Nur A. 2009. Elastic wave speeds and moduli in polycrystalline ice Ih, sI methane hydrate, and sII methane-ethane hydrate. *J. Geophys. Res.* 114:B02212
39. Helgerud MB, Circone S, Stern L, Kirby S, Lorenson TD. 2002. Measured temperature and pressure dependence of compressional and shear wave speeds in polycrystalline sII methane+ethane hydrate. *Proc. Intl. Conf. Gas Hydrates, 4th, Yokohama, Japan*, pp. 716–21. Tokyo: Keio Univ.
40. Helgerud MB, Waite WF, Kirby SH, Nur A. 2003. Measured temperature and pressure dependence of V_p and V_s in compacted, polycrystalline ice, Ih. *Can. J. Phys.* 81:81–87
41. Mork M, Schei G, Larsen R. 2000. NMR imaging study of hydrates in sediments. *Ann. N. Y. Acad. Sci.* 912:897–905

42. Dvorkin J, Helgerud MB, Waite WF, Kirby SH, Nur A. 2000. Introduction to physical properties and elasticity models. In *Natural Gas Hydrate: In Oceanic and Permafrost Environments*, ed. MD Max, pp. 245–60. Dordrecht, Netherlands: Kluwer Acad.
43. Waite WF, Stern LA, Kirby SH, Winters WJ, Mason DH. 2007. Simultaneous determination of thermal conductivity, thermal diffusivity and specific heat in sI methane hydrate. *Geophys. J. Int.* 169:767–74
44. Subramanian S. 2000. *Measurements of clathrate hydrates containing methane and ethane using Raman spectroscopy*. PhD thesis, Colo. Sch. Mines, Golden, Colo. 312 pp.
45. Ripmeester JA, Ratcliffe CI. 2000. The contributions of NMR spectroscopy to clathrate science. *J. Struct. Chem.* 40:654–62
46. Kini RA. 2002. *NMR Studies of Methane, Ethane, and Propane Hydrates: Structure, Kinetics, and Thermodynamics*. PhD thesis. Colo. Sch.Mines, Golden, Colo. 200 pp.
47. Koh CA, Sloan ED. 2007. Natural gas hydrates: recent advances and challenges in energy and environmental applications. *AIChE J.* 53:1636–43
48. Murshed MM, Kuhs WF. 2009. Kinetic studies of methane–ethane mixed gas hydrates by neutron diffraction and Raman spectroscopy. *J. Phys. Chem. B* 113:5172–80
49. Koh CA. 2002. Towards a fundamental understanding of natural gas hydrates. *Chem. Soc. Rev.* 31:157–67
50. Lehmkühler F, Paulus M, Sternemann C, Lietz D, Venturini F, et al. 2009. The carbon dioxide–water interface at conditions of gas hydrate formation. *J. Am. Chem. Soc.* 131:585–89
51. Thompson H, Soper AK, Buchanan P, Aldiwan N, Creek JL, Koh CA. 2006. Methane hydrate formation and decomposition: structural studies via neutron diffraction and empirical potential structure refinement. *J. Chem. Phys.* 124:164508–12
52. Udachin KA, Ratcliffe CI, Ripmeester JA. 2001. Structure, composition, and thermal expansion of CO_2 hydrate from single crystal X-ray diffraction measurements. *J. Phys. Chem. B* 105:4200–4
53. Udachin KA, Lu H, Enright GD, Ratcliffe CI, Ripmeester JA, et al. 2007. Single crystals of naturally occurring gas hydrates: the structures of methane and mixed hydrocarbon hydrates. *Angew. Chem. Int. Ed.* 46:8220–22
54. Udachin KA, Ripmeester JA. 1999. A complex clathrate hydrate structure showing bimodal guest hydration. *Nature* 397:4200–4
55. Ohno H, Strobel TA, Dec SF, Sloan ED, Koh CA. 2009. Raman studies of methane–ethane hydrate metastability. *J. Phys. Chem. A* 113:1711–16
56. Florusse LJ, Peters CJ, Schoonman J, Hester KC, Koh CA, et al. 2004. Stable low-pressure hydrogen clusters stored in a binary clathrate hydrate. *Science* 306:469–71
57. Strobel TA, Hester KC, Koh CA, Sum AK, Sloan ED. 2009. Properties of the clathrates of hydrogen and developments in their applicability for hydrogen storage. *Chem. Phys. Lett.* 478:97–109
58. van der Waals JH, Platteeuw JC. 1956. Clathrate solutions. *Adv. Chem. Phys.* 2:1–57
59. Wierzchowski SJ, Monson PA. 2007. Calculation of free energies and chemical potentials for gas hydrates using Monte Carlo simulations. *J. Phys. Chem. B* 111:7274–82
60. Zele SR, Lee S-Y, Holder GD. 1999. A theory of lattice distortion in gas hydrates. *J. Phys. Chem.* B 103:10250–57
61. Parrish WR, Prausnitz JM. 1972. Dissociation pressures of gas hydrates formed by gas mixtures. *Ind. Eng. Chem. Proc. Des. Dev.* 11:26–35
62. Ballard AL, Sloan ED. 2001. Hydrate phase diagrams for methane + ethane + propane mixtures. *Chem. Eng. Sci.* 56:6883–95
63. Subramanian S, Ballard AL, Kini R, Dec SF, Sloan ED. 2000. Structural transitions in methane plus ethane gas hydrates—Part I: upper transition point and applications. *Chem. Eng. Sci.* 55:5763–71
64. Jensen L, Thomsen K, von Solms N, Wierzchowski S, Walsh MR, et al. 2010. Calculation of liquid water-hydrate-methane vapor phase equilibria from molecular simulations. *J. Phys. Chem. B* 114:5775–82
65. Conde MM, Vega C, McBride C, Noya EG, Ramirez R, Sese LM. 2010. Can gas hydrate structures be described using classical simulations? *J. Chem. Phys.* 132:114503
66. Dohrn R, Peper S, Fonseca JMS. 2010. High-pressure fluid-phase equilibria: experimental methods and systems investigated (2000–2004). *Fluid Phase Equilib.* 288:1–54.
67. Fonseca JSM, Dohrn R, Peper S. 2011. High-pressure fluid-phase equilibria: experimental methods and systems investigated (2005–2008). *Fluid Phase Equilib.* 300:1–69

68. Sjöblom J, Øvrevoll B, Jentoft G, Lesaint C, Palermo T, et al. 2010. Investigation of the hydrate plugging and non-plugging properties of oil. *J. Dispers. Sci. Technol.* 31:1100–19
69. Taylor CJ, Dieker LD, Miller KT, Koh CA, Sloan ED. 2007. Micromechanical adhesion force measurements between tetrahydrofuran hydrate particles. *J. Colloid Interface Sci.* 306:255–61
70. Aman Z, Dieker L, Aspenes G, Sloan ED, Sum AK, Koh CA. 2010. Influence of model oil with surfactants and amphiphilic polymers on cyclopentane hydrate adhesion forces. *Energy Fuels* 24:5441–45
71. Boxall J. 2009. *Hydrate plug formation from <50% water content water-in-oil emulsions.* PhD thesis. Colo. Sch. Mines, Golden, Colo. 291 pp.
72. Boxall JA, Davies SR, Koh CA, Sloan ED. 2009. Predicting when and where hydrate plugs form in oil-dominated flowlines. *SPE Proj. Facil. Constr.* 4:80–86
73. Davies S. 2009. *The role of transport resistances in the formation and remediation of hydrate plugs*. PhD thesis. Colo. Sch. Mines, Golden, Colo. 289 pp.
74. Matthews PN, Notz PK. 2000. Flow loop experiments determine hydrate plugging tendencies in the field. *Ann. N.Y. Acad. Sci.* 912:330–38
75. Vysniauskas A, Bishnoi PR. 1983. A kinetic study of methane hydrate formation. *Chem. Eng. Sci.* 38:1061–72
76. Walsh MR, Koh CA, Sloan ED, Sum AK, Wu DT. 2009. Microsecond simulations of spontaneous methane hydrate nucleation and growth. *Science* 326:1095–98
77. Vatamanu J, Kusalik PG. 2006. Unusual crystalline and polycrystalline structures in methane hydrates. *J. Am. Chem. Soc.* 128:15588–89
78. Schicks JM, Ripmeester JA. 2004. Hydrate phases under moderate pressure and temperature conditions: kinetic versus thermodynamic products. *Angew. Chem. Int. Ed.* 43:3310–13
79. Kelland M. 2006. History of the development of low dosage hydrate inhibitors. *Energy Fuels* 20:825–47
80. Moridis GJ, Collett TS, Pooladi-Darwish M, Hancock S, Santamarina C, et al. 2010. Challenges, uncertainties and issues facing gas production from hydrate deposits in geologic systems. *SPE Unconv. Gas Conf., Pittsburgh*, SPE131792. Houston: Soc. Pet. Eng.
81. Moridis GJ, Sloan ED. 2007. Gas production potential of disperse low-saturation hydrate accumulations in oceanic sediments. *J. Energy Convers. Manag.* 48:1834–49
82. Gudmundsson JS, Parlaktuna M. 1992. *Storage natural gas at hydrate refrigerated conditions*. Presented at AIChE Spring Natl. Meet., New Orleans, LA
83. Stern LA, Circone S, Kirby SH, Durham WB. 2001. Anomalous preservation of pure methane hydrate at 1 atm. *J. Phys. Chem. B* 105:1756–62
84. Boswell R. 2009. Is gas hydrate energy within reach? *Science* 325(5943):957–58

Annual Review of Chemical and Biomolecular Engineering

Volume 2, 2011

Contents